VLBA Observations of Four Radio-Selected Dual AGNs in Stripe 82 Region

Wancheng Xu[1], Lang Cui[1], Xiang Liu[1], Tao An[2], Hongmin Cao[3], Pengfei Jiang[1], Luis C. Ho[4], Ning Chang[1], Xiaolong Yang[2], Yuling Shen[1], Guiping Tan[1], Zhenhua Han[5], Junhui Fan[6], and Ming Zhang[1]

1 Introduction and Targets

According to the galaxy hierarchical evolution theory, small galaxies assemble through mergers and interactions into progressively larger systems, eventually forming the massive galaxies and clusters we observe today. During galaxy mergers, tidal torques could trigger the accretion and feedback of central black holes and form dual active galactic nuclei (AGN). However, only a few dual AGNs have been confirmed through observations. Studying the emission properties of rare dual AGN can provide valuable insights into galaxy merging and black hole activations.

Previously, Fu et al. (2015a,b) found a group of dual-AGN candidates in Stripe 82 region by radio-optical imaging comparation and optical spectroscopy. The follow-up VLA C-band observations confirmed that four of the pairs were true dual AGN. These dual AGNs exhibit paired mJy-level compact radio morphologies and steep radio spectra in the VLA C-band observations (Figure 1 middle column). The separation in each pair is about 2.5~4.6 arcsec, corresponding to about 4.1~11.6 kpc. Through VLBI high-resolution imaging, we aim to reveal the milliarcsecond-scale radio emission properties of the four rare confirmed dual AGNs, and to investigate the effects of merging on the black holes and their host galaxies.

2 VLBA Observations

We observed the four confirmed dual AGNs using VLBA at 5 GHz in February, 2018 (project code: BL255). Our observations used multiple-phase-center mode which allows high-resolution imaging of each AGN within the primary beam area by adjusting the phase center. In addition, the phase-referencing technique allows us to detect the precise positions of central black holes. The observational data was calibrated in AIPS with traditional VLBA phase-referencing calibration process and imaged in DIFMAP through Gaussian model fitting with natural weight.

3 Results and Discussion

In eight components of the targets, our VLBA 5 GHz observations detected two pc-scale radio cores labelled J0051+0020B and J2300-0005A (Figure 1 side columns). The radio emission of the other six AGNs was resolved out in high-resolution imaging. We obtained the phase-referencing coordinates and 5 GHz flux densities of two VLBA-detected sources, and estimated their brightness temperatures and radio emission powers using formula (1) and (2), which are similar to those of typical jet-dominated AGNs. For the other six undetected sources, we provided their upper-limit values of these parameters (Table 1).

Based on the pc-scale radio emission properties of the targets, we analyzed the 5 GHz radio emission origins in detail for each source (Table 2). The VLBA flux densities represent the contribution of pc-scale compact jet of the targets. The proportion of radio emission originated from the corona is estimated using L_R/L_X~10^{-5}, based on the Chandra X-ray observational results, which should be ignored in most targets. The contribution of star formation is estimated through the 1.4 GHz luminosity, Hα luminosity and formula (3)-(4). The rest radio emission is thought to originate from extended jet and wind. The 5 GHz radio emission of almost all targets is jet-dominated, only J2206+0003B is probably dominated by star formation. Figure 2(a) shows the radio spectral shape of J2206+0003B.

The multiband study revealed a possible systematic X-ray deficit in our small dual-AGN sample (Figure 2b), which could be attributed to the merger-driven tidally induced effect. The analysis of X-ray hardness ratio (HR) indicates that the VLBA-detected sources may have a lower X-ray absorption (Figure 2c). Therefore, the X-ray deficit could also be caused by possibly viewing angle effect. In addition, the [O III] excess originated from star formation could also reduce the X-ray-to-[O III] luminosity ratio. But the distribution of the targets in Figure 4(d) does not show a different trend with general AGNs.

Two VLBA-detected sources have a significant (~10 mas) radio-optical position offset between their VLBA phase-referenced positions and Gaia positions (Figure 1). They both have significant astrometry excess noise (AEN) in Gaia DR3, similar to "Varstrometry" selected dual AGN. Their Gaia positions could be weighted centers of AGN and host galaxies, and their VLBA positions correspond to the location of the black hole. Their significant AEN could be caused by dark Gaia magnitudes and complex galaxy structures.

4 Future

The results of the emission properties in dual AGN need to be verified through larger-sample observations and analysis. To confirm and study interesting dual-AGN candidates which have significant radio-optical offsets, we have presented an EVN observational proposal to reveal the fine radio structures of two "Varstrometry" selected dual-quasar candidates with a redshift more than 0.5 (project code: EX010). The outstanding sensitivity and high resolution of EVN are helpful in achieving the above scientific goals.

(1) $T_b = 1.22 \times 10^{12}(1+z)\frac{S_\nu}{\theta^2\nu^2}$

(2) $L_\nu = 4\pi d_L^2 \frac{S_\nu}{(1+z)^{1+\alpha}}$

(3) $SFR_{\mathrm{H}\alpha} = \frac{L_{\mathrm{H}\alpha}}{5.37\times10^{42}\ \mathrm{erg/s}}$

(4) $SFR_{1.4\mathrm{GHz}} = \frac{fL_{1.4\mathrm{GHz}}}{1.81\times10^{21}\ \mathrm{W/Hz}}$

Reference

Barnes & Hernquist 1996, ApJ, 471, 115
Condon et al. 1982, ApJ, 252, 102
Condon 1992, ARA&A, 30, 575
Deller et al. 2011, PASP, 123, 275
Di Matteo et al. 2005, Natur, 433, 604
Fu et al. 2015a, ApJ, 799, 72
Fu et al. 2015b, ApJL, 815, L6
Gross et al. 2019, ApJ, 883, 50
Güdel & Benz 1993, ApJL, 405, L63
Ho 2002, ApJ, 564, 120
Hogg et al. 2002, ArXiv
Hopkins et al. 2003, ApJ, 599, 971
Liu et al. 2013, ApJ, 762, 110
Murphy et al. 2011, ApJ, 737, 67
Springel et al. 2005, Natur, 435, 629
Van Wassenhove et al. 2012, ApJL, 748, L7

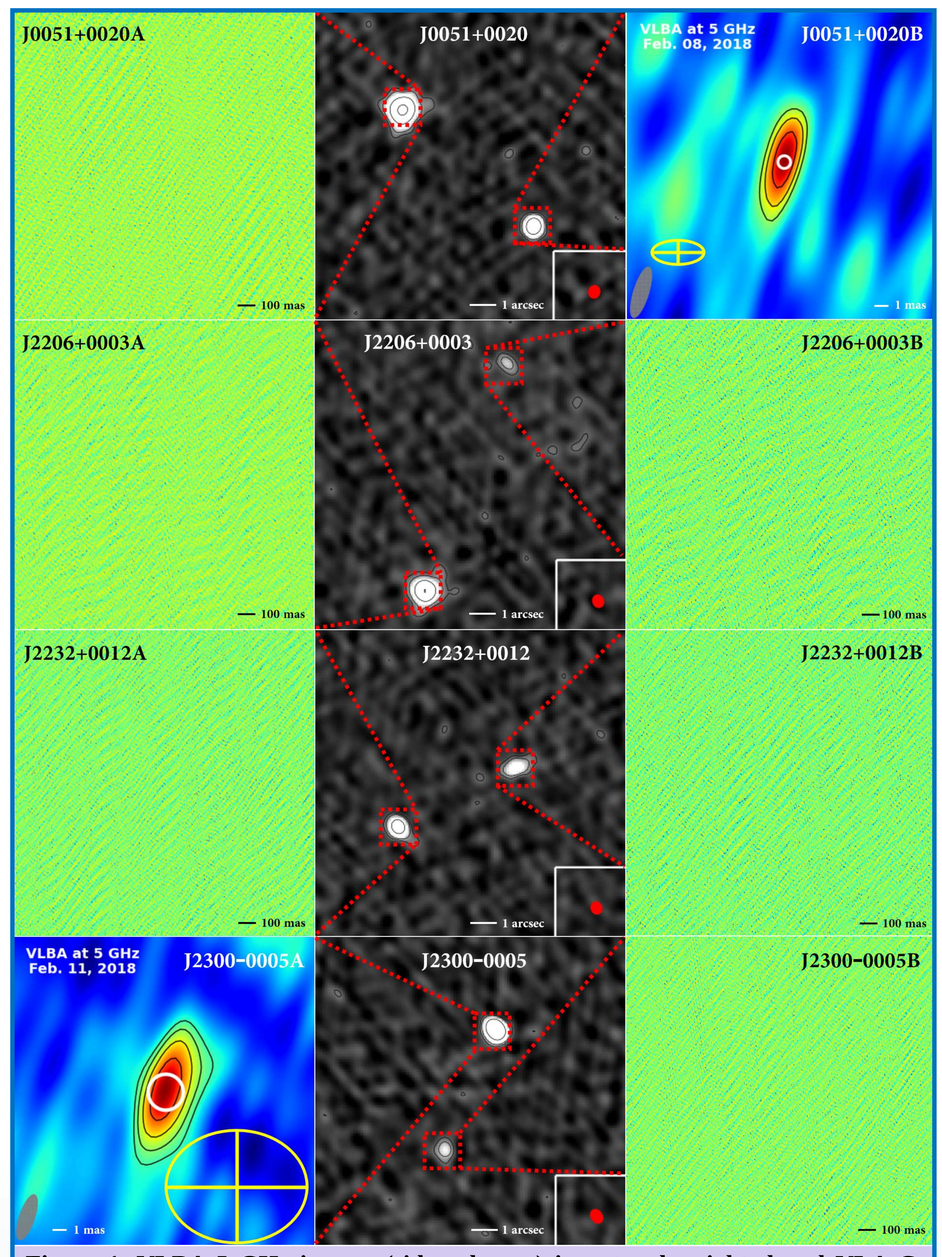

Figure 1. VLBA 5 GHz images (side columns) in natural weighted and VLA C-band images (middle column) of the targets. In the middle column, the black contours are at (+3, +6, +24, +96)×σ, and the beam is in the bottom right corner (Fu et al. 2015b). For two VLBA-detected sources J0051+0020B and J2300-0005A, their Gaussian-fitting images are provided, with black contours at (+1, +$\sqrt{2}$, +2, +2$\sqrt{2}$)×3σ and model-fitting core sizes (white circle). The yellow crosses and ellipses represent the ±1σ region around the Gaia positions. No reliable signal was found within the range of ±1 arcsec for the other VLBA-undetected sources, so only dirty images are provided.

Source	$S^{\mathrm{VLA}}_{5\mathrm{GHz}}$ (mJy)	$S^{\mathrm{VLBA}}_{5\mathrm{GHz}}$ (mJy)	θ (mas)	log T_b (K)	log $L_{5\mathrm{GHz}}$ (W/Hz)
J0051+0020A	1.11±0.03	<0.15	>3.79	<5.74	<21.72
J0051+0020B	0.36±0.02	0.20±0.03	0.84±0.24	~7.21	~21.77
J2206+0003A	0.72±0.02	<0.14	>3.44	<5.78	<20.85
J2206+0003B	0.11±0.04	<0.11*	>3.44	<5.67	<20.75
J2232+0012A	0.31±0.02	<0.16	>3.57	<5.86	<22.35
J2232+0012B	0.19±0.03	<0.16	>3.57	<5.87	<22.35
J2300−0005A	0.56±0.02	0.40±0.05	2.37±0.18	~6.64	~22.49
J2300−0005B	0.08±0.03	<0.08*	>3.61	<5.57	<21.88

Table 1. Radio emission properties of the targets. The VLA 5 GHz flux density is estimated based on the VLA C-band observations of the targets (Fu et al. 2015b). Our VLBA observations provide pc-scale flux densities (or 6σ upper limits), angular scales, brightness temperatures and radio emission powers of the targets. We are using VLA 5 GHz flux density to replace their flux density upper limits for two sources marked "*", because of the sensitivity limitation of the VLBA.

Source	Compact jet	Extended jet+wind	Corona	Star formation
J0051+0020A	<13%	>64%	...	<23%
J0051+0020B	~56%	>25%	...	<19%
J2206+0003A	<20%	>47%	~6%	<27%
J2206+0003B	?	?	...	<72%
J2232+0012A	<51%	>49%	...	...
J2232+0012B	<81%	>19%	...	...
J2300−0005A	~71%	~29%	...	...
J2300−0005B	?	?	...	...

Table 2. The 5 GHz radio emission origins of the targets. The compact jet proportion is from the VLBA 5 GHz detection (see Table 1). The contribution of corona and star formation are estimated based on X-ray luminosity and Hα luminosity of the targets (Gross et al. 2019). The rest radio emission is thought to originate from extended jet and wind. The ellipsis represents the contribution is less than 3% and should be ignored. The question mark represents the unknown proportion based on current observations.

Citation: Wancheng Xu et al 2024 ApJ 969 36 **DOI:** 10.3847/1538-4357/ad463b

Figure 2. Multiband emission properties of the targets.

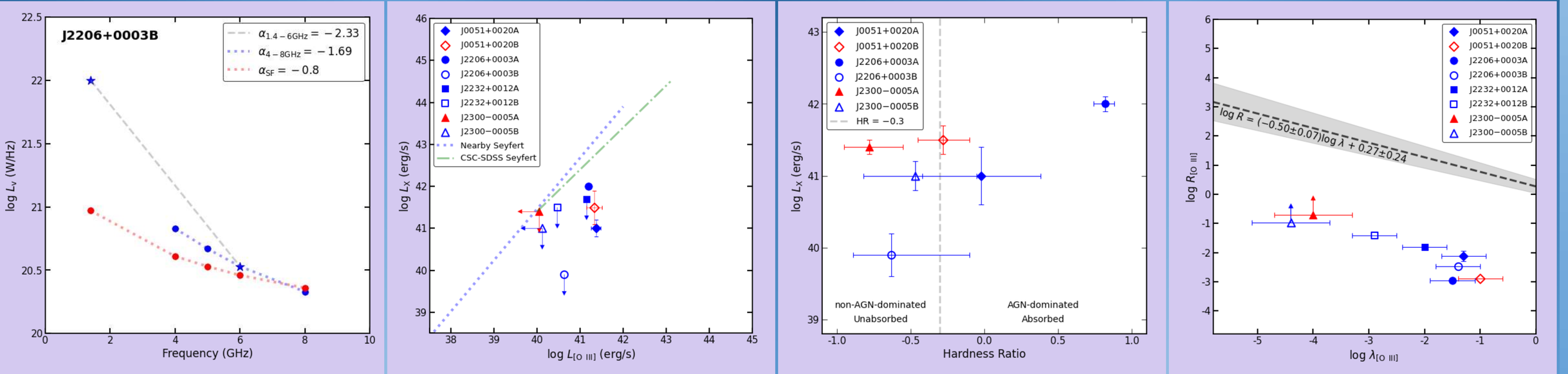

(a) Radio emission luminosity (L_ν) of J2206+0003B vs. observational frequency.

(b) Rest-frame 2~10 keV X-ray luminosity (L_X) vs. [O III] emission-line luminosity ($L_{[\mathrm{O\ III}]}$).

(c) X-ray luminosity (L_X) vs. Hardness ratio (HR).

(d) Radio loudness ($R_{[\mathrm{O\ III}]}$) vs. Eddington ratio ($\lambda_{[\mathrm{O\ III}]}$).